Cleavage of Disulfide-Bridged Stalk Domains during Shedding of Angiotensin-Converting Enzyme Occurs at Multiple Juxtamembrane Sites†

Sylva L. U. Schwager,‡ Anthony J. Chubb,‡ Zenda L. Woodman,‡ Lisa Yan,§ Reinhard Mentele,|| Mario R. W. Ehlers,⊥ and Edward D. Sturrock*,‡,#

Department of Medical Biochemistry and MRC/UCT Liver Research Centre, Department of Medicine, University of Cape Town Medical School, Observatory 7925, South Africa, Molecular Simulations, Inc., San Diego, California 92121-3752, Abteilung für Klinische Chemie und Klinische Biochemie, Ludwig-Maximilians-Universität, D-80336 München, Germany, and Restoragen, Inc., Lincoln, Nebraska 68524

Received May 23, 2001; Revised Manuscript Received August 9, 2001

ABSTRACT: Shedding of the ectodomain of angiotensin-converting enzyme (ACE) and numerous other membrane-anchored proteins results from a specific cleavage in the juxtamembrane (JM) stalk, catalyzed by "sheddases" that are commonly activated by phorbol esters and inhibited by peptide hydroxamates such as TAPI. Sheddases require a stalk of minimum length and steric accessibility. However, we recently found that substitution of the ACE stalk with an epidermal growth factor (EGF)-like domain from the low-density lipoprotein receptor (LDL-R) did not abolish shedding; cleavage of the ACE−JMEGF chimera occurred at a Gly−Phe bond in the third disulfide loop of the EGF domain. We have now constructed two additional stalk chimeras, in which the native stalk in ACE was replaced with the EGF domain from factor IX (ACE−JMfIX) and with a cysteine knot motif (ACE−JMmin23). Like the ACE−JMEGF chimera, the ACE−JMfIX and −JMmin23 chimeras were also shed, but mass spectral analysis revealed that the cleavage sites were adjacent to, rather than within, the disulfide-bonded domains. Homology modeling of the LDL-R EGF domain revealed that the third disulfide loop is larger and more flexible than the equivalent loop in the factor IX EGF domain. Similarly, the NMR structure of the Min-23 motif is highly compact. Hence, cleavage within a disulfide-bonded domain appears to require an unhindered loop. Interestingly, unlike wild-type ACE and the ACE−JMEGF and −JMmin23 chimeras, shedding of the ACE−JMfIX chimera was not stimulated by phorbol or inhibited by TAPI, but instead was inhibited by 3,4-dichloroisocoumarin, indicating the activity of an alternative sheddase. In summary, the ACE shedding machinery is highly versatile, but an accessible JM sequence, in the form of a flexible stalk or an exposed loop within or adjacent to a folded domain, appears to be required. Moreover, alternative sheddases are recruited, depending on the nature of the JM sequence.

The release of membrane-bound proteins by proteolysis has been identified as a key event in the regulation of many cellular processes, including cell−cell and cell−matrix adhesion, modulation of the number of receptors, and generation of systemically active cytokines and enzymes (*1*, *2*). The shedding of cell surface proteins is catalyzed in most cases by a group of disintegrin metalloproteases of the ADAMs family that are inhibited by hydroxamic acid-based compounds, such as TAPI and TAPI-2 (*2*, *3*). However, evidence for alternative sheddases has been presented (*4*−*6*).

Angiotensin-converting enzyme (ACE)[1] is a membrane-bound dipeptidyl carboxypeptidase involved in blood pressure regulation (*1*). Somatic ACE is expressed at tissue−fluid interfaces throughout the body and is also found in most bodily fluids, such as blood plasma, seminal plasma, and urine (*7*, *8*). The soluble isoform of ACE is produced by proteolytic shedding of membrane-bound ACE (*9*, *10*), but its physiological significance has not been elucidated (*11*).

† This work was supported by grants from the Volkswagen Foundation to E.D.S. and M.R.W.E., the Wellcome Trust to E.D.S., the National Research Foundation (NRF) to E.D.S., and the Medical Research Council of South Africa. Z.L.W. was the recipient of an NRF scholarship.

* To whom correspondence should be addressed: Department of Medical Biochemistry, University of Cape Town Medical School, Observatory 7925, South Africa. Telephone: (021) 406 6312. Fax: (021) 447 7669. E-mail: sturrock@curie.uct.ac.za.

‡ Department of Medical Biochemistry, University of Cape Town Medical School.

§ Molecular Simulations, Inc.

|| Ludwig-Maximilians-Universität.

⊥ Restoragen, Inc.

MRC/UCT Liver Research Centre, Department of Medicine, University of Cape Town Medical School.

[1] Abbreviations: ACE, angiotensin-converting enzyme; WT-ACE, wild-type testis ACE; ACE−JMEGF and −JMFIX, juxtamembrane mutants with a substitution of the wild-type stalk with an EGF-like domain from the LDL receptor and human factor IX, respectively; APP, amyloid precursor protein; CHO, Chinese hamster ovary; CSB, cystine-stabilized β-sheet; EC, extracellular; EGF, epidermal growth factor; Hip-His-Leu, hippuryl-L-histidyl-L-leucine; LDL, low-density lipoprotein; MALDI-TOF, matrix-assisted laser desorption ionization time-of-flight; PBS, phosphate-buffered saline; PCR, polymerase chain reaction; phorbol ester, phorbol 12,13-dibutyrate; TAPI, TNF-α protease inhibitor; TM, transmembrane; TNF-α, tumor necrosis factor-α.

10.1021/bi011063c CCC: $20.00
Published on Web 11/29/2001

Proteolytic shedding occurs within the "stalk", a stretch of amino acid residues connecting the transmembrane (TM) region to the extracellular (EC) domain of ectoproteins, including ACE. The structure of this region is poorly characterized and was investigated as a possible common requirement for cleavage specificity and recognition by "sheddases". Significant deletions or substitutions of the ACE stalk are tolerated by sheddases, but a minimum stalk length has been identified as a requirement for cleavage (*12*). Sheddases may require an unhindered stretch of amino acid residues, because many noncleavable proteins, such as the integrin β-subunit and P- and E-selectins, contain highly disulfide-linked, likely conformationally constrained stalks (*13*, *14*).

Previously, we investigated the effect of a cysteine-rich domain proximal to the ACE TM region, by substituting an epidermal growth factor (EGF)-like domain from the low-density lipoprotein receptor (LDL-R) for the ACE stalk region (ACE−JMEGF mutant). Surprisingly, the EGF-like stalk was cleaved, although the extent of shedding was strongly reduced because cleavage occurred within a disulfide bridge and the ectodomain remained tethered to the TM domain via this link (*15*). EGF-like domains are characterized by a compact structure formed by three disulfide bonds, of which the first two form a disulfide β-cross structure (*16*), while the third loop contains two β-turns; cleavage of the ACE−JMEGF chimera occurred within this loop. Thus, even constrained, disulfide-bonded domains may contain sequences that are sufficiently exposed to offer cleavage sites for the sheddase.

In this report, the requirement for an exposed loop for cleavage was investigated further by constructing mutants in which the ACE stalk was replaced with another EGF-like domain (from factor IX) with a shorter, more constrained third loop, and with a highly compact, synthetic disulfide-linked peptide called Min-23. Expression of the ACE−JMfIX and ACE−JMmin23 chimeras in CHO cells revealed that both were shed into the conditioned medium. Analysis of the stalk cleavage sites revealed that unlike in the ACE−JMEGF chimera, cleavage occurred more distally, between the inserted disulfide-bonded domains and the ectodomain, indicating that the factor IX EGF-like domain and the Min-23 domain were resistant to direct cleavage by ACE-shedding proteases. The ACE shedding machinery appears to be highly versatile in terms of cleavage site sequences, but a minimum requirement is an exposed or unhindered sequence of minimum length between the EC domain and the membrane. Such exposed sequences may be within or adjacent to otherwise compact, folded domains.

MATERIALS AND METHODS

Construction of Expression Vectors and CHO Cell Transfection. The ACE stalk was replaced with an EGF-like domain that has a known crystal structure. The EGF domain from the clotting factor, factor IX, was selected because its three-dimensional structure has been extensively characterized (*17*) and it is 42% identical with the LDL-R EGF-like domain used in our previous studies (*15*). Construction of the mutant pLEN-ACEfIX was performed by using a two-stage PCR strategy. The sequence encoding Asp93−Glu129 of human factor IX, which represents the EGF-like homology domain, was amplified using suitable primers. Similarly, the sequence encoding Arg651−Ser687, representing the TM and cytoplasmic domains of wild-type testis ACE (WT-ACE), was amplified. The two products, containing overlapping segments, were then co-amplified using two flanking primers. The fusion product that was generated was digested with *Eco*RI and *Cla*I and ligated into the pLEN-ACE vector as described previously (*12*, *15*) to generate pLEN-ACEfIX.

pLEN-ACEmin23 encodes human testis ACE in which the wild-type stalk is replaced with a cystine-stabilized β-sheet motif (*18*), and was constructed as follows. Two hybrid DNA fragments were generated by the amplification of nucleotides 1853−1990 and 2067−2221 of the complete testis ACE cDNA sequence. The hybrid inner primers on either side of the deleted ACE sequence comprised the complete Min-23 DNA sequence and were complementary to one another at their 5′ ends. The two DNA fragments were further amplified using the outer primers to produce a 360 bp fragment with an *Eco*RI restriction enzyme site introduced at nucleotide 1984, as in the construct pLEN-ACE-JMΔ24 (*12*), facilitating assembly of the final construct, pLEN-ACEmin23, as described for pLEN-ACEfIX, above.

The expression vectors pLEN-ACEfIX and pLEN-ACE-min23 were stably expressed in CHO cells as described previously (*12*).

Analysis of Release Kinetics and Cleavage Sites. After selection for stable transfectants, kinetic analyses of rates of accumulation of soluble (released) ACE activity and changes in membrane-bound ACE activity were performed in the presence and absence of 1 μM phorbol 12,13-dibutyrate, 100 μM TAPI (peptide hydroxamate, a gift from R. A. Black, Immunex Corp.), or 200 μM 3,4-dichloroisocoumarin (DCI), as described previously (*4*, *15*). Identification of the stalk cleavage sites in the released (soluble) proteins was performed as described previously (*15*).

Fluorescent Immunocytochemistry. Transfected cells were seeded on sterile coverslips in six-well plates, cultured to 60% confluency, and incubated in DME medium supplemented with 20 mM Hepes (pH 7.3), 2% fetal calf serum, and 40 μM $ZnCl_2$ overnight. Cells were fixed in 3% paraformaldehyde (PFA) in PBS for 15 min and permeabilized with 0.1% Triton X-100 for 5 min. To determine the amount of extracellular membrane-bound ACE, cells were fixed in PFA and not exposed to Triton X-100. The immunostaining procedure included blocking nonspecific binding of antisera using 3% bovine serum albumin in PBS, incubation in rabbit polyclonal antibody directed against human kidney ACE (*19*), and detection of bound antibodies with fluorescein isothiocyanate (FITC)-conjugated goat anti-rabbit IGG. For nuclear staining, cells were exposed to 2 μM propidium iodide (PI) for 10 min and coverslips were mounted onto glass microscope slides using MOWIOL. Samples were viewed using a confocal laser scanning microscope (Leica DM IRBE) where images were captured using the 488 and 568 nm excitation wavelengths for the FITC and PI signals, respectively. Laser power and photomultiplier settings were identical for all images.

Homology Modeling of the ACE−JMEGF Chimera. A homology model of the entire EGF-like domain of the ACE−JMEGF chimera was constructed as follows.

(i) Identification of the Template. Homologous sequences of the ACE−JMEGF chimera were searched against the

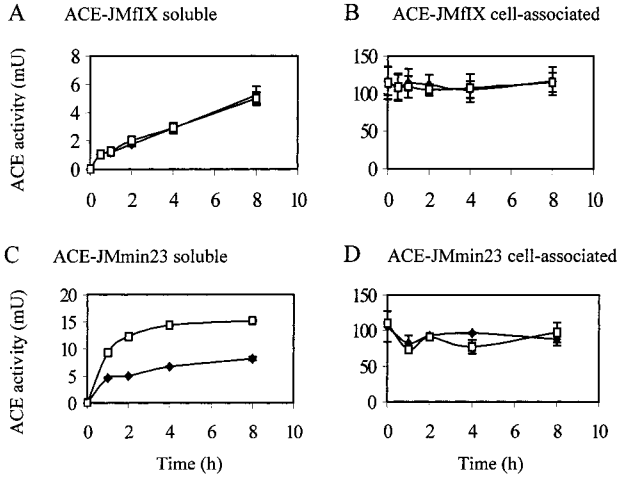

FIGURE 1: Kinetics of solubilization (shedding) (A and C) and changes in cell-associated levels (B and D) of ACE−JMfIX (A and B) and ACE−JMmin23 (C and D) chimeras expressed in CHO cells. Stably transfected cells were grown in complete medium, in the presence (□) or absence (◆) of phorbol ester. Medium samples (soluble activity) and detergent lysates (cell-associated activity) were collected at the indicated time points and assayed with the ACE substrate Hip-His-Leu. The results are means ± standard deviations of four separate experiments, each performed in duplicate.

Protein Data Bank (PDB) using FASTA and PSI-BLAST. EGF-like domains were aligned by predominantly manual means, taking into account pronounced sequence features such as the conserved disulfide linkages.

(ii) Construction of Homology Models. Models based on the alignments were constructed using the Modeler 5.0 program (*20*).

RESULTS

Expression in CHO Cells and Kinetics of Release. The ACE−JMfIX and ACE−JMmin23 chimeras were designed to support the hypothesis that stalk regions with a defined secondary structure do not completely inhibit cleavage by sheddase activity but that cleavage within folded domains requires an exposed loop (*15*). To achieve this, an EGF-like domain from factor IX that was 42% identical to the LDL-R EGF-like domain, used in our previous study, was substituted for the stalk region of WT-ACE. In the case of the ACE−JMmin23 chimera, a highly compact, synthetic disulfide-linked peptide of 23 amino acids (Min-23) was substituted.

The extent of release of the ACE−JMfIX and ACE−JMmin23 chimeras and the accumulation of soluble protein in the conditioned medium over an 8 h period were poor (Figure 1), consistent with the kinetic data for the ACE−JMEGF chimera (*15*). Phorbol ester stimulation was absent for the ACE−JMfIX chimera, but resulted in a reproducible 2−3-fold increase in the initial rate of release for the ACE−JMmin23 chimera, compared to 3-fold increases for ACE−JMEGF and WT-ACE release (Figures 1 and 2A) (*15*). As in the case of the ACE−JMEGF chimera, there was no significant change in levels of the membrane-bound ACE−JMfIX and ACE−JMmin23 chimeras (Figures 1 and 2A) after phorbol treatment.

Inhibition of the release of the membrane-bound ACE−JMmin23 chimera by TAPI was comparable to that observed for WT-ACE and the ACE−JMEGF chimera, whereas the ACE−JMfIX chimera was unaffected (Figure 2B) (*15*).

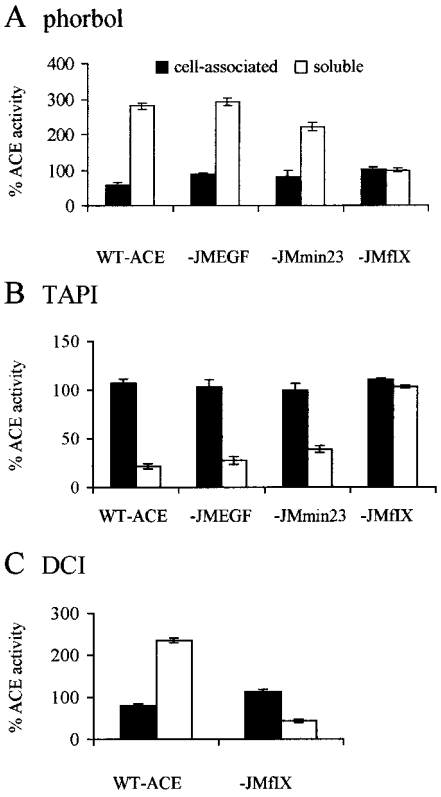

FIGURE 2: Effects of phorbol ester, TAPI, and DCI on levels of cell-associated and soluble ACE proteins. Transfected cells were incubated for 4 h in medium containing 1 μM phorbol ester (A), 100 μM TAPI (B), or 200 μM DCI (C). Samples of cell lysates (black bars) or medium (white bars) were assayed with the substrate Hip-His-Leu. Results are expressed as a percentage relative to control (no treatment), taken as 100% in each case (not shown), and are means ± standard deviations of three independent samples.

Previous work involving mutants that were not inhibited by peptide hydroxamates (*4*, *5*) revealed that shedding was inhibited by the serine protease inhibitor DCI, as opposed to WT-ACE release that is stimulated by DCI. Incubation of cells expressing the ACE−JMfIX chimera with DCI inhibited release of soluble protein by ∼60%, whereas the extent of release of WT-ACE was increased 2−3-fold (Figure 2C).

Determination of the Juxtamembrane Cleavage Sites. Denatured, reduced, and vinylpyridine-protected soluble ACE−JMfIX and ACE−JMmin23 chimeras were digested with endoproteinase Lys-C and fractionated by HPLC, and peptides were analyzed by MALDI-TOF mass spectrometry. The spectra of the Lys-C peptides revealed $[M + H]^+$ ions at *m*/*z* 1261.3 and 1576.7 for the ACE−JMfIX and ACE−JMmin23 chimeras, respectively, which corresponded to the theoretical masses of the peptides of Leu614−Pro623 (1262.4) and Leu614−Leu626 (1576.6), respectively (Table 1). These peptides were identified as the C-terminal peptides for the ACE−JMfIX and −JMmin23 chimeras as they were the only peptides not containing a C-terminal Lys-C residue. Moreover, the LGWPQYNWTP C-terminal peptide of the ACE−JMfIX chimera was identified from an enriched HPLC fraction via N-terminal sequencing. We therefore concluded that the cleavage site for the ACE−JMfIX chimera was between Pro623 and Asn624, and that for the ACE−JMmin23 chimera was between Leu626 and Met627 (Figure 3).

Table 1: Observed $[M + H]^+$ Ions Generated from HPLC-Fractionated Peptides Derived from Endoproteinase Lys-C Digests of Released (shed) ACE−JMfIX and ACE−JMmin23 Chimeras

		observed *m/z*	
peptide residues	calcd *m/z*	ACE−JMfIX	ACE−JMmin23
557−567	1176.4	1176.7	1175.2
598−613	1951.2	1952.2	1951.0
614−623	**1262.4**	**1261.3**[a]	
614−626	**1576.6**		**1576.7**

[a] The identity of the peptide was confirmed by N-terminal sequencing. Bold characters indicate C-terminal peptides.

Subcellular Localization of the ACE−JMfIX Chimera. ACE shedding has been localized to the cell surface (*10*, *21*). However, an ACE mutant with a single point mutation in the stalk region appears to be cleaved by a distinct serine-like protease in the endoplasmic reticulum (*5*). To examine whether shedding of the ACE−JMfIX chimera occurs inside the cell or at the cell surface, we immunostained cells expressing the ACE−JMfIX chimera and WT-ACE cells with a polyclonal antibody that recognizes the N-terminal ectodomain of ACE. Both WT-ACE and the ACE−JMfIX chimera were localized predominantly at the cell surface (Figure 4A,B), although a smaller intracellular pool of the enzyme was observed in the permeabilized cells (Figure 4C,D). Thus, the ACE−JMfIX mutant, like WT-ACE, was processed efficiently to the cell surface. Furthermore, ACE activity was only detected in the detergent-rich phase of ACE−JMfIX cell lysates treated with Triton X-114 (data not shown), indicating that the soluble from of the mutant was not released inside the cell. These data are consistent with the cell surface being the major site of cleavage and release of the ACE−JMfIX chimera, as shown previously for WT-ACE.

Homology Modeling of the LDL-R EGF-like Domain. To investigate the different cleavage sites of the ACE−JMEGF and ACE−JMfIX chimeras, we performed homology modeling studies on the entire EGF domain of the LDL receptor. The PDB was searched for sequences homologous to the LDL-R EGF-like domain. Fibrillin (1EMN) was 32% identical and was chosen as a template for this modeling study. The alignments of the EGF-like domain sequences used in the modeling are shown in Figure 3; the C-terminal domain of 1EMN gave the best alignment with the ACE−JMEGF chimera, given that they have the same number of residues between the last disulfide bridge (Cys5 and -6). Human factor IX has a short loop between the fifth and sixth Cys residues, whereas the ACE−JMEGF chimera and 1EMN have loops that are longer by three residues. Five homology models of the EGF-like domain of the ACE−JMEGF chimera were created using Modeler 5.0 based on the sequence alignment and satisfaction of spatial restraints derived from structural templates. The model with the lowest energy is shown in Figure 5, compared with the factor IX crystal structure (1IXA).

The homology-modeled structure clearly showed the disulfide β-cross motif characteristic of EGF-like domains. The C-terminal disulfide loop comprised two β-turns, one a type II turn and the other a type I. The first turn was at Asp651−Phe653 with the ACE sheddase cleavage site located in this turn, at the Gly652−Phe653 bond. The second

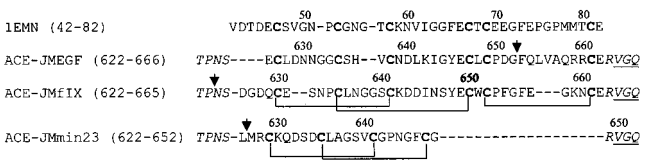

FIGURE 3: Sequence of the EGF-like domain in the ACE−JMEGF chimera and alignment with related domains in 1EMN, factor IX, and Min-23. In the ACE chimeric proteins, numbering is consecutive with respect to the testis ACE sequence (*34*), and flanking ACE sequences, including the start of the TM domain (underlined), are in italics. The respective sequence positions in the ACE−JMEGF, −JMfIX, and −JMmin23 chimeras (E626−E662, D626−E662, and L626−G648, respectively) correspond to E296−E332, D4−E38, and L1−G23 for LDL-R EGF, factor IX EGF, and Min-23, respectively. The sheddase cleavage sites in the ACE−JMEGF, −JMfIX, and −JMmin23 chimeras are denoted with arrows. The conserved cysteine residues are in bold, and the disulfide bonding pattern is indicated.

β-turn before Cys661, including Arg659 and Arg660, was directly homologous to the turn at Pro36 and Met37 in 1EMN. The three residues, including the peptide bond that was cleaved, in the ACE−JMEGF model and the homologous region of the factor IX crystal structure are shown in a ball-and-stick representation (Figure 5A). In factor IX, the aromatic rings of Phe654 and Phe656 faced outward, whereas in the ACE−JMEGF chimera, the phenyl ring of Phe653 was positioned inside the loop, likely because the C-terminal disulfide loop is longer by three residues. The phenyl ring had the same conformation in the template 1EMN and resided within the loop. In contrast, in factor IX the phenyl ring of Phe654 could not be rotated to face into the loop, because the loop was shorter and more constrained. Therefore, the scissile Gly652−Phe653 peptide bond in the ACE−JMEGF chimera was sterically more accessible than the homologous (uncleaved) bond (Gly655−Phe656, Figure 3) in factor IX.

DISCUSSION

Naturally occurring EGF-like domains are generally resistant to cleavage by sheddases (*13*, *22*). This is either due to the secondary structure of these domains or, as suggested previously (*15*), because cleavage does occur but the protein remains tethered to the membrane by a disulfide bond. The unusual cleavage of an EGF-like domain in the ACE−JMEGF chimera (*15*) prompted us to investigate further the structural constraints on substrates cleaved by the ACE-shedding proteases. The complete atomic structure of the LDL receptor has not been determined, and thus, we employed homology modeling to determine the three-dimensional structure of its N-terminal EGF-like domain. Moreover, a second ACE−EGF mutant was constructed using the factor IX EGF-like domain to test the notion that the length of the third disulfide loop determines cleavage susceptibility.

The ACE−JMfIX protein accumulated on the cell surface (Figure 4) with inefficient release of the processed form into the culture medium, consistent with our hypothesis that a stalk with a compact disulfide-bonded domain reduces but does not completely inhibit ectodomain shedding. MALDI-TOF analysis indicated that the cleavage occurred distal to the EGF-like domain at the Pro623−Asn624 bond and not within the C-terminal disulfide loop as was the case with

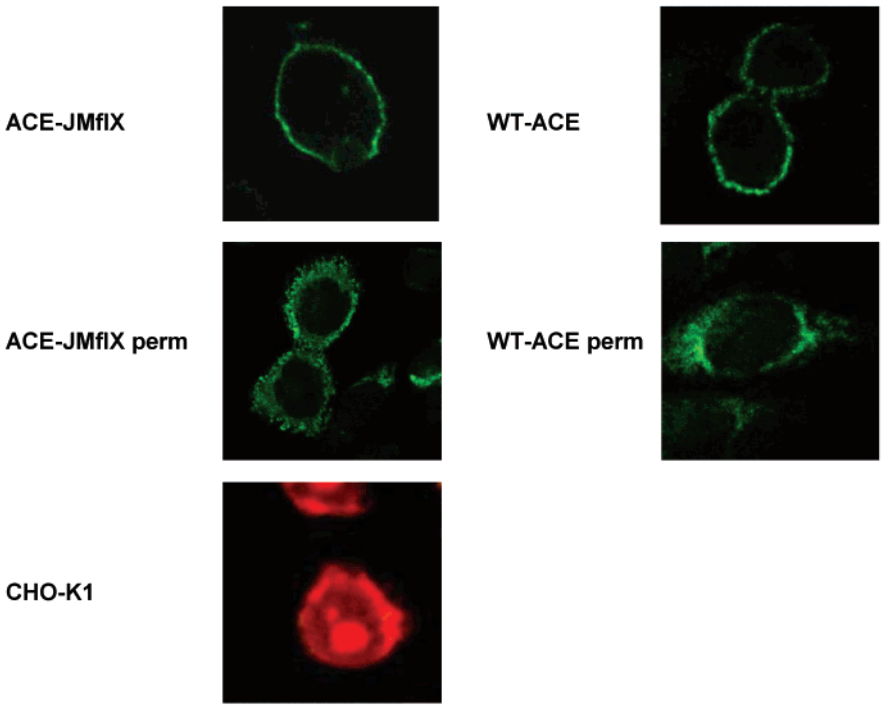

FIGURE 4: Immunofluorescence localization of WT-ACE and the ACE−JMfIX chimera in CHO-K1 cells. Following incubation with the ACE antibody, cells were stained with FITC IgG and propidium iodide, and analyzed by confocal laser scanning microscopy. For the WT-ACE and ACE−JMfIX preparations, only the FITC channel is shown. However, for the CHO-K1 cells, the FITC and propidium iodide channels have been overlaid to show specificity of staining in WT-ACE and ACE−JMfIX cells. All images were captured under identical conditions using a 63× water-immersion objective lens (ACE-JMFIXperm and WT-ACEperm indicate cultures exposed to Triton X-100).

the ACE−JMEGF chimera. Comparison of the LDL-R and factor IX EGF domains (Figure 5A) revealed that the C-terminal disulfide loop of the ACE−JMfIX stalk sequence represents a relatively short span of residues between the TM domain of ACE and the C-terminal β-sheet of the inserted EGF domain, and is sterically more constrained than the homologous loop in the ACE−JMEGF chimera.

We propose an explanation for the intra-EGF domain proteolytic cleavage of the ACE−JMEGF protein based on the homology model of its EGF domain. Compared to the factor IX crystal structure, the homology model revealed that the LDL-R EGF domain had a larger and more exposed C-terminal disulfide loop (between the fifth and sixth Cys residues) (Figure 4A). It is particularly notable that the aromatic ring of Phe653 in the ACE−JMEGF chimera is accommodated within the C-terminal disulfide loop, whereas the aromatic rings of Phe654 and Phe656 in the factor IX EGF domain are oriented to the outside of the loop. The homology model is supported by solution NMR studies completed while this work was in progress (*23*, *24*). Hence, it appears that cleavage at the Gly652−Phe653 bond in the ACE−JMEGF chimera was facilitated by the more exposed, sterically unhindered structure of this loop, whereas the equivalent bond in the ACE−JMfIX chimera (Gly655−Phe656) was too constrained to allow cleavage. Instead, cleavage of the ACE−JMfIX protein occurred more distally, "upstream" of the EGF domain.

However, an analysis of the different cleavage sites in the ACE−JMEGF and ACE−JMfIX chimeras is complicated by two considerations. First, in contrast to the shedding of the ACE−JMEGF chimera and also WT-ACE, shedding of the ACE−JMfIX protein was not stimulated by phorbol ester or inhibited by TAPI, indicating the participation of an alternative sheddase. Moreover, shedding of the ACE−JMfIX chimera was inhibited by DCI, suggesting that an unidentified serine protease may be involved, rather than one of the ADAMs protease that have been identified as sheddases. Therefore, it is difficult to assign general cleavage requirements to a specific "ACE sheddase", since clearly more than one protease is involved. Nevertheless, regardless of the number and identities of sheddases, general rules for the ACE shedding machinery can be developed. For example, although the shedding machinery is versatile, cleavage of compactly folded stalk domains is constrained (as evidenced by the ACE−JMfIX and ACE−JMmin23 chimeras; see below), and an accessible stalk of minimum length is required (*12*).

The second consideration when analyzing the cleavage sites in ACE−JMEGF and −JMfIX chimeras is the precise nature of the steric hindrance within the third loop in the ACE−JMfIX chimera; i.e., does it result from (a) the shorter length, (b) the orientation of Phe656, or (c) the presence of a second Phe residue (Phe654)? This cannot be definitively answered on the basis of the data presented here, but it is instructive to compare the results of a third mutant (ACE−JMmin23) in which the ACE stalk sequence was replaced with a 23-residue cystine-stabilized β-sheet (CSB) motif derived from the squash trypsin inhibitor (EETI II) (*18*) (Figure 4B). This peptide (Min-23) contains the two characteristic disulfides, a triple-stranded β-sheet, a 3_{10}-helix, and two β-turns of the CSB motif (Figure 5B). Min-23 folds in a native-like fashion, indicating that the CSB can be considered an autonomous folding unit, and hence was chosen as a replacement for the native ACE stalk sequence.

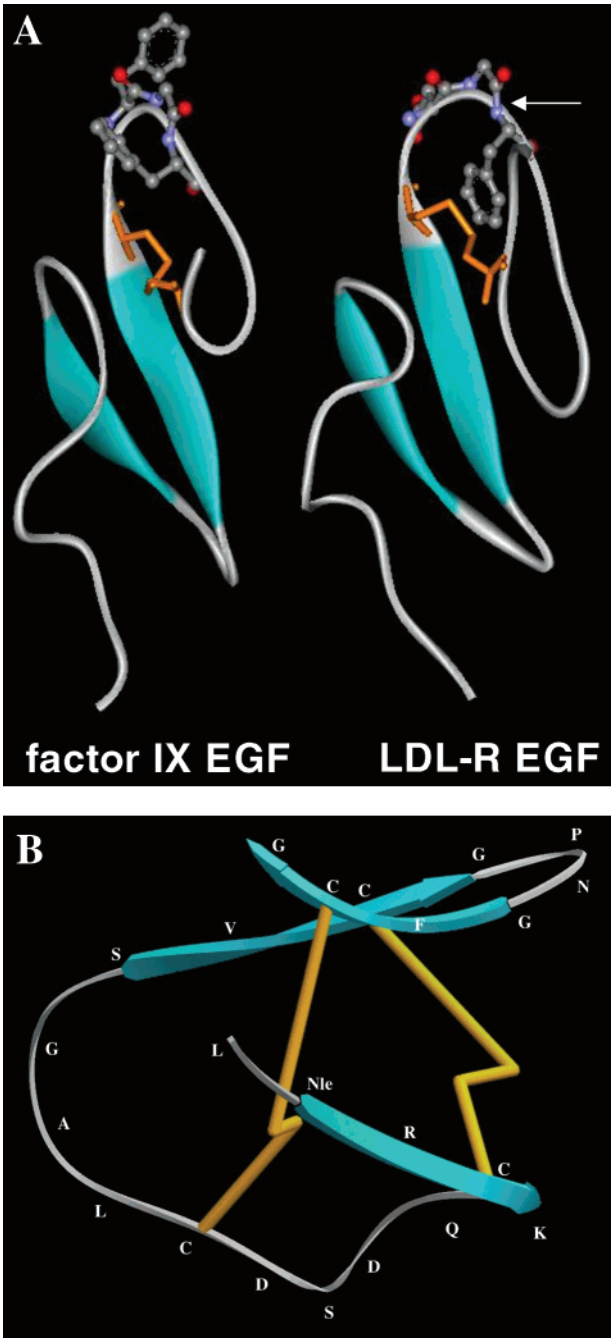

FIGURE 5: Structures of the compactly folded disulfide-linked domains used for the ACE juxtamembrane mutants. (A) View of the three-dimensional model of the ACE−JMEGF and ACE−JMfIX chimeras. The three residues at the cleavage site are shown in a ball-and-stick representation, and the disulfide bridges are in yellow. The Gly−Phe bond where cleavage occurs in the ACE−JMEGF chimera is indicated with an arrow. The ACE−JMEGF structure was generated with Modeler 5.0 (MSI) and the factor IX accessed from the Protein Data Bank (entry 1IXA). (B) A ribbon diagram of the Min-23 peptide and cystine-stabilized β-sheet motif. The disulfide bridges are displayed in yellow and the β-strands in blue. Atom coordinates were obtained from L. Chiche (Centre de Biochimie Structurale, UMR5048 CNRS-Université Montpellier I, Montpellier, France), and the figure was created using SETOR (*35*).

As noted for both ACE−JMEGF and −JMfIX chimeras, release of the EC domain of the ACE−JMmin23 protein was comparatively inefficient. Analysis of the stalk cleavage site revealed that, as for the ACE−JMfIX mutant, the ACE−JMmin23 mutant was cleaved distally, between the Min-23 and EC domains. The Min-23 domain contains two disulfide loops, N- and C-terminal, where the former extends from C629 to C641 and the latter from C635 to C647 (Figure 3). The C-terminal loop can be viewed as being analogous to the C-terminal loop in EGF, and notably, the Min-23 loop also has 11 residues as in the EGF domain of the ACE−JMEGF chimera. Moreover, in the Min-23 loop there is the sequence CGPNGF, which is very similar to C-PDGF in JMEGF. However, the aromatic ring of Phe646 in Min-23 also faces the outside of the loop, analogous to Phe656 in the ACE−JMfIX chimera. Hence, the absence of cleavage at the Gly655−Phe656 bond in the ACE−JMfIX protein is not likely the result of a second aromatic side chain at Phe654, but instead, as in the ACE−JMmin23 chimera, more likely due to the tight turns and outward orientation of Phe656. Comparison of ACE−JMfIX and −JMmin23 chimeras also suggests that the length of the loop is not critical per se, but rather the tightness of the folds, resulting from the shorter loop length in the former and the crossed disulfide motif in the latter (Figure 5A,B). In light of the compact structure of the Min-23 motif (Figure 5B), the data add further support to the proposal that the ACE sheddases require an exposed or unhindered sequence (or loop) of minimum length and/or flexibility to allow access by the protease active sites.

It is reasonable to propose that the selection of the cleavage site is dependent not on the chemical characteristics of side chains but rather on the degree of access offered. Our results are consistent with recent studies involving ACE and other membrane proteins. Eyries et al. described a point mutation in the stalk of somatic ACE (Pro1199 to Leu, five residues N-terminal to the Arg1203−Ser1204 cleavage site) that significantly enhanced the rate of shedding (*25*). Two-dimensional structure analysis revealed the likely presence of a seven-residue loop immediately C-terminal to Pro1199 that contains the native cleavage site, which is bounded by more constrained β-sheet and α-helical sequences N- and C-terminally, respectively (*25*). Substitution of Leu for Pro1199 may therefore extend the length and accessibility of this loop and thereby enhance cleavage by the sheddase. Similarly, on the basis of chimeras involving the exchange of stalk sequences between two membrane proteins that are not usually shed (gp130 and LIF), Althoff et al. (*26*) concluded that susceptibility to shedding is governed principally by the degree of "disorder" of the juxtamembrane domain. Thus, whether there is a defined stalk or a folded domain with a sufficient degree of disorder, an emerging consensus is that cleavage by sheddases requires access to an unhindered or flexible loop of sufficient length. Cleavage efficiency increases in proportion to increasing stalk or loop flexibility and disorder.

This view is consistent with a model proposed for the TACE active site, which clearly requires access to part of the juxtamembrane region of the substrate protein that is in an extended geometry (*27*, *28*). Moreover, the TACE active site model also makes a provision for distal interactions between the sheddase and the substrate (*28*), which can be interpreted as contacts with an unidentified recognition or activation motif, as proposed by Sadhukhan et al. (*29*) and us (*10*). Sheddase requirements for both an accessible juxtamembrane sequence and a distal recognition motif are not mutually exclusive. However, the identity and precise

role of the putative recognition motif remain to be defined. It is possible that such a motif plays a more prominent role in the activity of one or more of the ACE sheddases than it does in TACE.

The identities of the ACE sheddases remain unknown. On balance, the evidence suggests that there may be a primary enzyme as well as one or more additional enzymes (*4*). These enzymes appear not to be identical with TACE (*5*, *30*), which is more constrained by stalk characteristics (*31*, *32*), but it is very likely that the primary ACE sheddase is also a member of the family of peptide hydroxamate-inhibitable ADAMs proteases (*25*, *28*, *33*). As noted, shedding of the ACE−JMfIX chimera was not stimulated by phorbol ester and was not inhibited by TAPI, key characteristics of ADAMs proteases (*28*, *33*). Instead, shedding of the ACE−JMfIX protein was inhibited by DCI, as was reported previously for the stalk glycosylation mutant ACE-JGL (*4*) and for an ACE mutant with a point mutation in the stalk (Asn631Gln) (*5*). However, in contrast to the Asn631Gln mutant, which was shed by an intracellular protease (*5*), we found that cleavage and release of the ACE−JMfIX chimera occurred predominantly at the cell surface. These data indicate that alternative sheddases are recruited, depending on stalk characteristics. This may explain, in part, why the ACE shedding machinery appears to be so versatile.

ACKNOWLEDGMENT

We thank A. Kristina Downing for helpful discussions and allowing us access to the coordinates for the LDL-R EGF-AB pair. We appreciate K. R. Acharya's useful comments and the assistance of J. Swaminathan in generating the structure of EETI II. We also thank E. van der Merwe for kindly performing the confocal immunofluorescence microscopy.

REFERENCES

1. Ehlers, M. R., and Riordan, J. F. (1991) *Biochemistry 30*, 10065−10074.
2. Hooper, N. M., Cook, S., Laine, J., and LeBel, D. (1997) *Biochem. J. 324* (Part 1), 151−157.
3. Arribas, J., Coodly, L., Vollmer, P., Kishimoto, T. K., Rose-John, S., and Massague, J. (1996) *J. Biol. Chem. 271*, 11376−11382.
4. Schwager, S. L., Chubb, A. J., Scholle, R. R., Brandt, W. F., Mentele, R., Riordan, J. F., Sturrock, E. D., and Ehlers, M. R. (1999) *Biochemistry 38*, 10388−10397.
5. Alfalah, M., Parkin, E. T., Jacob, R., Sturrock, E. D., Mentele, R., Turner, A. J., Hooper, N. M., and Naim, H. Y. (2001) *J. Biol. Chem. 276*, 21105−21109.
6. Schlondorff, J., Lum, L., and Blobel, C. P. (2001) *J. Biol. Chem. 276*, 14665−14674.
7. Erdos, E. G., and Skidgel, R. A. (1987) *Lab. Invest. 56*, 345−348.
8. Lanzillo, J. J., Stevens, J., Dasarathy, Y., Yotsumoto, H., and Fanburg, B. L. (1985) *J. Biol. Chem. 260*, 14938−14944.
9. Beldent, V., Michaud, A., Wei, L., Chauvet, M. T., and Corvol, P. (1993) *J. Biol. Chem. 268*, 26428−26434.
10. Woodman, Z. L., Oppong, S. Y., Cook, S., Hooper, N. M., Schwager, S. L., Brandt, W. F., Ehlers, M. R., and Sturrock, E. D. (2000) *Biochem. J. 347* (Part 3), 711−718.
11. Esther, C. R., Marino, E. M., Howard, T. E., Machaud, A., Corvol, P., Capecchi, M. R., and Bernstein, K. E. (1997) *J. Clin. Invest. 99*, 2375−2385.
12. Ehlers, M. R., Schwager, S. L., Scholle, R. R., Manji, G. A., Brandt, W. F., and Riordan, J. F. (1996) *Biochemistry 35*, 9549−9559.
13. Kahn, J., Ingraham, R. H., Shirley, F., Migaki, G. I., and Kishimoto, T. K. (1994) *J. Cell Biol. 125*, 461−470.
14. Kishimoto, T. K., O'Connor, K., Lee, A., Roberts, T. M., and Springer, T. A. (1987) *Cell 48*, 681−690.
15. Schwager, S. L., Chubb, A. J., Scholle, R. R., Brandt, W. F., Eckerskorn, C., Sturrock, E. D., and Ehlers, M. R. (1998) *Biochemistry 37*, 15449−15456.
16. Harrison, P. M., and Sternberg, M. J. (1996) *J. Mol. Biol. 264*, 603−623.
17. Rao, Z., Handford, P., Mayhew, M., Knott, V., Brownlee, G. G., and Stuart, D. (1995) *Cell 82*, 131−141.
18. Heitz, A., Le Nguyen, D., and Chiche, L. (1999) *Biochemistry 38*, 10615−10625.
19. Ehlers, M. R., Chen, Y. N., and Riordan, J. F. (1991) *Protein Expression Purif. 2*, 1−9.
20. Sali, A., and Blundell, T. L. (1993) *J. Mol. Biol. 234*, 779−815.
21. Oppong, S. Y., and Hooper, N. M. (1993) *Biochem. J. 292* (Part 2), 597−603.
22. Chen, A., Engel, P., and Tedder, T. F. (1995) *J. Exp. Med. 182*, 519−530.
23. Malby, S., Pickering, R., Sara, S., Smallridge, R., Linse, S., and Downing, A. K. (2001) *Biochemistry 40*, 2555−2563.
24. Saha, S., Boyd, J., Werner, J. M., Knott, V., Handford, P. A., Campbell, I. D., and Downing, A. K. (2001) *Structure 9*, 451−456.
25. Eyries, M., Michaud, A., Deinum, J., Agrapart, M., Chomilier, J., Kramers, C., and Soubrier, F. (2001) *J. Biol. Chem. 276*, 5525−5532.
26. Althoff, K., Mullberg, J., Aasland, D., Voltz, N., Kallen, K., Grotzinger, J., and Rose-John, S. (2001) *Biochem. J. 353*, 663−672.
27. Maskos, K., Fernandez-Catalan, C., Huber, R., Bourenkov, G. P., Bartunik, H., Ellestad, G. A., Reddy, P., Wolfson, M. F., Rauch, C. T., Castner, B. J., Davis, R., Clarke, H. R., Petersen, M., Fitzner, J. N., Cerretti, D. P., March, C. J., Paxton, R. J., Black, R. A., and Bode, W. (1998) *Proc. Natl. Acad. Sci. U.S.A. 95*, 3408−3412.
28. Black, R. A., and White, J. M. (1998) *Curr. Opin. Cell Biol. 10*, 654−659.
29. Sadhukhan, R., Sen, G. C., Ramchandran, R., and Sen, I. (1998) *Proc. Natl. Acad. Sci. U.S.A. 95*, 138−143.
30. Sadhukhan, R., Santhamma, K. R., Reddy, P., Peschon, J. J., Black, R. A., and Sen, I. (1999) *J. Biol. Chem. 274*, 10511−10516.
31. Arribas, J., Lopez-Casillas, F., and Massague, J. (1997) *J. Biol. Chem. 272*, 17160−17165.
32. Buxbaum, J. D., Liu, K. N., Luo, Y., Slack, J. L., Stocking, K. L., Peschon, J. J., Johnson, R. S., Castner, B. J., Cerretti, D. P., and Black, R. A. (1998) *J. Biol. Chem. 273*, 27765−27767.
33. Schlondorff, J., and Blobel, C. P. (1999) *J. Cell Sci. 112*, 3603−3617.
34. Ehlers, M. R., Fox, E. A., Strydom, D. J., and Riordan, J. F. (1989) *Proc. Natl. Acad. Sci. U.S.A. 86*, 7741−7745.
35. Evans, S. V. (1993) *J. Mol. Graphics 11*, 134−138.

BI011063C